DOI: 10.1002/ejic.201100286

^{29}Si NMR Shielding Calculations Employing Density Functional Theory, Focussing on Hypervalent Silicon Compounds

Van An Du,[a] Gregor N. Stipicic,[b] and Ulrich Schubert*[a]

Keywords: Silicon / ^{29}Si NMR spectroscopy / Density functional calculations / Hypervalent compounds

^{29}Si NMR chemical shifts of 41 silicon-containing compounds (14 tetra-, 10 penta- and 17 hexacoordinate compounds) were calculated by employing DFT using the gauge including atomic orbital (GIAO) formalism and compared to experimental values. The hybrid B3LYP functional, the generalized gradient approximation functional (GGA) BPW91 and the *meta*-GGA functional HCTH407 were used in conjunction with the 6-31G(d,p) and 6-311+G(2d) basis sets and a locally dense basis set [6-311G+(2d) on Si and 6-31G(d,p) on all other atoms]. The HCTH407/6-311+G(2d) level of theory consistently performed best with a mean average error (MAE) of 5.9 ppm between calculated and experimental chemical shifts over the entire test set (4.4, 5.7 and 7.9 ppm for tetra-, penta- and hexacoordinate compounds, respectively). The choice of a suitable basis set had a much larger influence on the accuracy of the results than the choice of functional. Additional calculations for some outliers with the 6-311++G(2df,2pd) basis set yielded only small improvements, whereas the economically attractive, locally dense basis set (LDBS) yielded an MAE of 6.5 ppm with the HCTH407 functional over the entire test set after correction of systematic errors. For a subset of compounds, GIAO-HF and MP2 ab initio calculations were performed yielding more accurate results than the DFT calculations (MAEs for HF, MP2 and HCTH407 were 3.9, 4.6 and 5.6 ppm, respectively) but required roughly two orders of magnitude more CPU time.

Introduction

Predicting the observable quantities of NMR spectra from first principles is of great interest, and numerous methods have been developed for the calculation of nuclear magnetic shielding[1,2] since the fundamental formulation by Ramsey.[3] The gauge including atomic orbital (GIAO) approach in conjunction with the coupled Hartree–Fock (CHF) method was a breakthrough for NMR chemical shift calculations.[4] It has been extended to DFT,[5,6] which has proven highly successful as an alternative to ab initio methods and generally yields useful results, even in more challenging cases such as transition metal compounds,[7] which are known to exhibit strong correlation effects.[8] ^{29}Si NMR shielding calculations by ab initio and DFT methods were used as an accurate tool for the prediction of chemical shifts in tetracoordinate silanes,[9] silane derivatives,[10] silanols[11] and organosiloxanes.[12] Triply bonded compounds such as disilynes (RSi≡SiR) were the subject of a computational study by Apeloig et al.[13] who showed that DFT with the HCTH407[14] functional exhibits a performance comparable to second-order many-body perturbation theory (MP2).[15] Recently, Rankin et al. demonstrated that ^{29}Si-^{1}H spin–spin coupling constants in organoalkoxysilanes can also be successfully predicted.[16] Experimentally, ^{29}Si NMR shifts have the characteristics to display large variations with local structure, involving the first and second shells of their neighbours as pointed out by Heine et al.[9] Although the silicon atoms in common silicon-containing molecules are tetracoordinate, hypervalent (i.e. five- and six-coordinate) silicon compounds are entirely different. Investigations of the mechanisms of their formation and structure both in the solid state and in solution (e.g. by NMR) have led to an improved understanding of their properties.[17–19]

In this contribution, the results of a DFT study on the calculation of ^{29}Si NMR shieldings carried out with a database of 41 molecules are presented, with a strong focus on penta- and hexacoordinate silicon compounds. The need of this study arose from our desire to use ^{29}Si NMR shielding calculations to aid in the interpretation of NMR spectra of hypervalent silicon compounds, such as those in ref.[20], where initial calculations showed large deviations between experimental data and calculated chemical shifts.

Results and Discussion

The selection of molecules for this study consists of 41 compounds with 44 distinct ^{29}Si NMR shifts (see Figure 1 for some examples; structural formulae of all compounds can be found in the Supporting Information). Compounds **1**–**14** contain at least one tetracoordinate silicon atom [including the smallest molecule considered in the present

---

[a] Institute of Materials Chemistry, Vienna University of Technology
Getreidemarkt 9, 1060 Vienna, Austria
[b] Institute of Applied Synthetic Chemistry, Vienna University of Technology
Getreidemarkt 9, 1060 Vienna, Austria

Supporting information for this article is available on the WWW under http://dx.doi.org/10.1002/ejic.201100286.

© 2011 Wiley-VCH Verlag GmbH & Co. KGaA, Weinheim

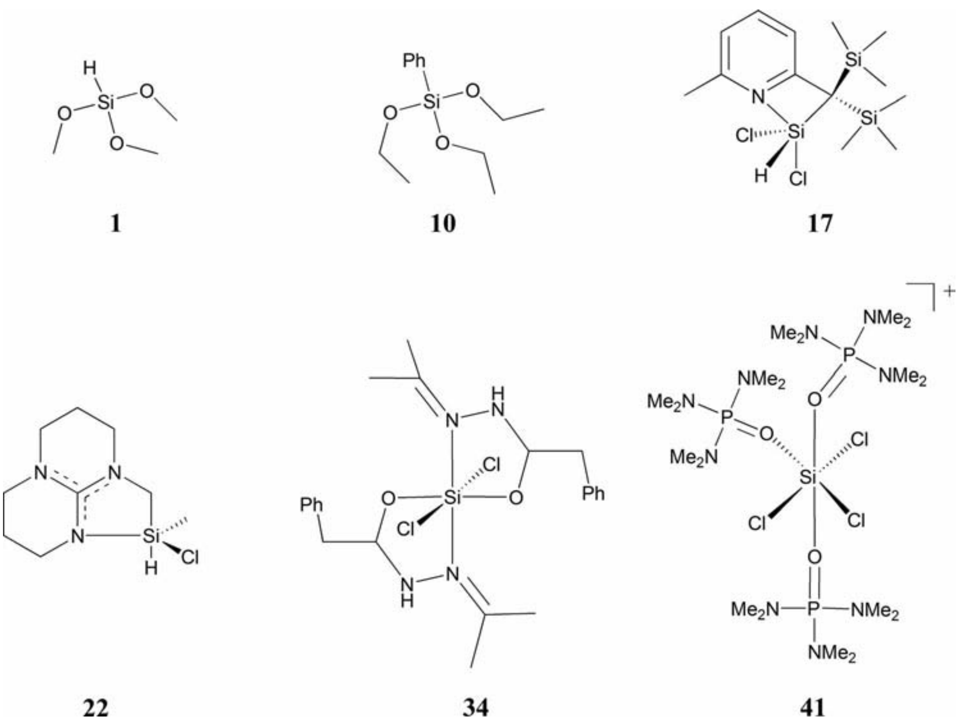

Figure 1. Structural formulae of the six largest outliers.

study, trimethoxysilane (**1**)], and **15**–**25** each exhibit one pentacoordinate silicon atom. The remainder of the compounds (**26**–**41**) feature a hexacoordinate silicon atom. Compound **41** consists of 91 atoms and is the largest molecule studied. The majority of the experimental chemical shifts used for comparison were recorded with $CDCl_3$ as a solvent. Experimental shifts relative to TMS range from δ = +22.9 to –188.7 ppm (Table 5). In case of the penta- and hexacoordinate molecules, the selection was guided by the availability of crystal structures as an unambiguous starting point for geometry optimizations and by the intention to investigate compounds with a high degree of structural diversity and different chemical shifts. Among the 41 molecules considered, all species except two (dianionic **36** and cationic **41**) are neutral.

For economic reasons, we preferred a larger database of molecules with different structural motifs to a larger survey of different density functionals in conjunction with a smaller database, in order to facilitate the identification of cases where theory yields inaccurate predictions. Our main concern was to find a suitable level of theory for ^{29}Si NMR shielding calculations with broad applicability to a range of different penta- and hexacoordinate compounds. The majority of the molecules investigated were medium to large, which is in contrast to the usual practice of selecting small molecules for benchmarking purposes.

We will discuss deviations between calculated chemical shifts and experimental values in terms of mean absolute error (MAE). Where $\delta calc_i$ = calculated NMR shift and $\delta expt_i$ = experimental NMR shift.

$$\mathbf{MAE} = \frac{1}{n}\sum_{i=1}^{n}|\delta calc_i - \delta expt_i|$$

For the entire database of 41 molecules (the different subsets are discussed below), the HCTH407/6-311+G(2d) level of theory yielded the best results. Data obtained with the hybrid B3LYP functional in conjunction with the 6-31G(d,p) and LDBS basis sets were more accurate than those obtained with the same basis sets and the HCTH407 functional. The pure BPW91 functional performs worst by a small margin regardless of basis set (Figure 2). Although the superiority of the HCTH407 functional is in agreement with the results obtained by Apeloig et al.[13] on a small set of disilynes, the hybrid B3LYP functional performs better than the pure BPW91 functional in the present study. The results obtained with the LDBS (see Computational Details) are strikingly better than those obtained with 6-31G(d,p) alone. This is of particular significance for calculations on large molecules because of the potentially dramatic reduction in cost [e.g. the calculations for compound **41** employ 853, 871 and 1217 basis functions with the 6-31G(d,p), locally dense and 6-311+G(2d) basis sets, respectively]. Additionally, it is immediately obvious from Figure 3 and Table 1 that the differences between the results for the LDBS and the 6-311G+(2d) basis are systematic. They are easily corrected by using the linear equation obtained from the linear regression (e.g. for HCTH407/LDBS, this leads to a reduction of the MAE from 8.0 to 6.5 ppm).

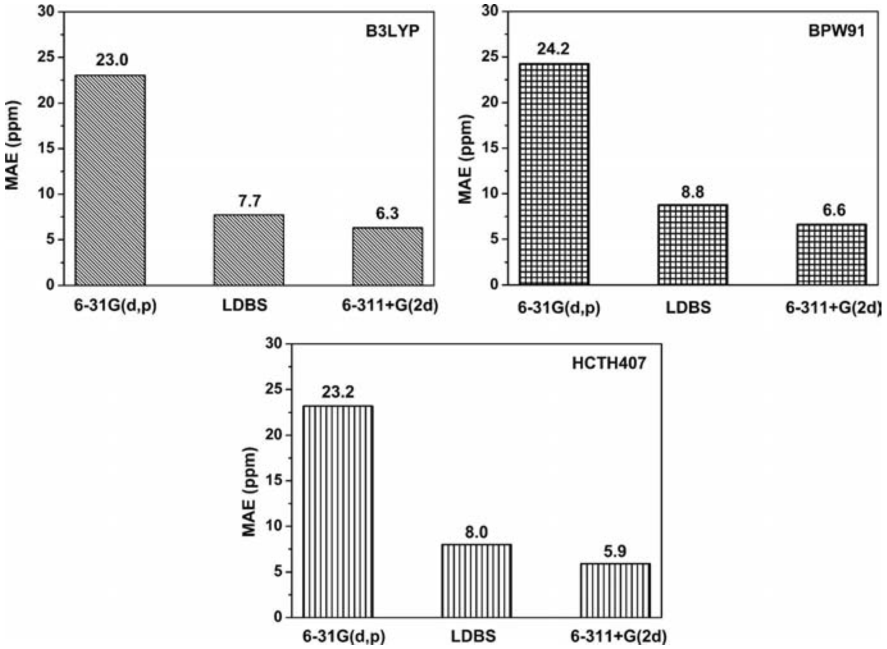

Figure 2. MAE between calculated and experimental chemical shifts for all 41 compounds at the given level of theory.

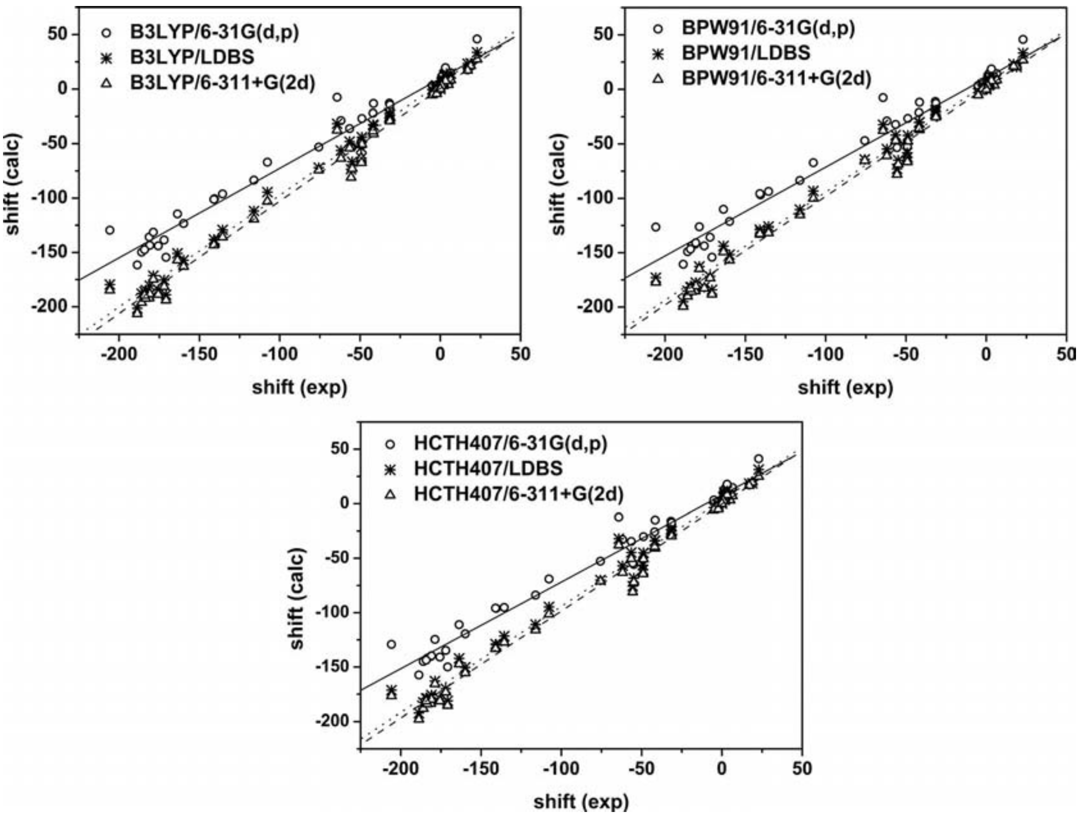

Figure 3. Plot of calculated vs. experimental chemical shift. Linear regressions are indicated.

Although the use of such relatively unbalanced basis sets might not be aesthetically pleasing from a theoretical perspective, it has also been used with success in a recent study by Morris et al.[21]

If the three classes of silicon-containing molecules (i.e. silane derivatives, penta- and hexacoordinate compounds, Table 2) are considered separately, the following trends are evident: for the small 6-31G(d,p) basis set, a modest agree-

Table 1. Parameters of the linear regression between experimental and calculated ^{29}Si chemical shift for all silicon-containing compounds. A = y intercept, B = slope, R = correlation coefficient.

Method and basis set	A	B	R
B3LYP/6-31G(d,p)	9.676 ± 2.209	0.823 ± 0.021	0.984
B3LYP/LDBS	5.339 ± 1.772	1.027 ± 0.017	0.993
B3LYP/6-311+G(2d)	0.478 ± 1.773	1.032 ± 0.017	0.994
BPW91/6-31G(d,p)	10.421 ± 2.280	0.817 ± 0.022	0.983
BPW91/LDBS	5.175 ± 1.888	0.994 ± 0.018	0.992
BPW91/6-311+G(2d)	1.731 ± 1.834	0.998 ± 0.018	0.993
HCTH407/6-31G(d,p)	7.868 ± 2.075	0.797 ± 0.020	0.985
HCTH407/LDBS	3.177 ± 1.820	0.974 ± 0.017	0.992
HCTH407/6-311+G(2d)	–0.304 ± 1.789	0.982 ± 0.017	0.993

ment with experimental values (regardless of the density functional used) is only found for the tetracoordinate silane derivatives (compounds **1**–**14**), whereas the results obtained for penta- and especially hexacoordinate compounds are discouraging. It is worth noting that Rankin et al.[16] obtained surprisingly good results when calculating ^{29}Si-^{1}H spin–spin coupling constants at the B3LYP/6-31G level of theory. Regarding ^{29}Si NMR shielding calculations, the results of our study clearly show that this apparently favourable behaviour of the small 6-31G(d,p) basis set does not extend to the penta- and hexacoordinate compounds. The LDBS already offers a dramatic improvement at a very small additional computational cost. Employment of the larger, but still computationally tractable 6-311+G(2d) basis set on all atoms results in further improvements and furnishes satisfactory results for both tetracoordinate and hypervalent pentacoordinate compounds.

For the six outliers with seven distinct chemical shifts (Figure 1), the geometries resulting from additional geometry optimizations at the most accurate level of theory identified above [i.e. HCTH407/6-311+G(2d), with a MAE of 16.7 ppm for the outliers] were used for the ^{29}Si NMR shielding calculations at the same level of theory in order to rule out the introduction of potential errors by using different levels of theory for geometry optimization and subsequent ^{29}Si NMR shielding calculations. The influence of changes in the structural parameters (including rovibrational effects) on the latter has been discussed in refs.[9,22–24] Although relatively large changes can be observed in individual cases, they are not systematic, as the overall MAE actually increases (Table 6).

Additionally, ^{29}Si NMR shielding calculations for the outliers were carried out with the even larger 6-311++G(2df,2pd) basis set on all atoms in order to measure the influence of basis set quality on the convergence of the obtained results. The mean absolute observed change for all seven distinct chemical shifts is less than 1.3 ppm, and the MAE increases slightly to 17.9 ppm (Table 6).

In a final attempt to reduce the large deviations from experiment for the six outliers, geometry optimizations and shielding calculations with HCTH407/6-311+G(2d) were carried out in conjunction with the integral equation formalism polarized continuum model (IEF-PCM)[25–27] in order to model the influence of the solvent. This approach results in an improved MAE of 14.8 ppm (Table 6).

The large deviations from experiment observed for the outliers are thus neither a result of different levels of theory used for geometry optimization and ^{29}Si NMR shielding calculations, nor insufficient quality of the employed basis sets nor negligence of solvent effects. Considering that three molecules with an Si–H bond can be found among the outliers, it is worth pointing out that Heine et al.[28] noted less satisfactory results when calculating chemical shifts of silanes with increasing numbers of hydrogen atoms bound to the silicon atom. The other molecules displaying a large error between experiment and theory do not share any obvious commonalities.

For the smallest compounds (**1**–**10**, **22**), GIAO-HF and MP2 ab initio calculations were carried out with the LDBS (see Table 3). For this subset, both HF and MP2 calculations yielded better results (with MAEs of 3.9 and 4.6 ppm) than the DFT calculations (with the best MAE of 5.6 ppm

Table 3. ^{29}Si NMR chemical shifts relative to TMS of molecules **1**–**10** and **22** and absolute isotropic shielding constants for TMS.

	Exp. shift	HF/LDBS	MP2/LDBS
1	–54.9	–60.6	–53.5
2	1.6	3.1	4.2
3	–2.5	1.1	1.7
4	–49.3	–52.9	–55.7
5	5.0	4.8	6.4
6	18.9	18.8	23.6
7	6.5	8.5	11.4
8	–5.1	–2.4	–1.0
9	17.0	16.1	25.7
10	–55.6	–64.1	–58.5
22	–49.1	62.8	–58.6
Tetramethylsilane	0	389.7	373.1

Table 2. MAE in ppm of calculated chemical shifts for silane derivatives, penta- and hexacoordinate compounds, respectively.

	B3LYP			BPW91				HCTH407	
	6-31G(d,p)	LDBS	6-311+G(2d)	6-31G(d,p)	LDBS	6-311+G(2d)	6-31G(d,p)	LDBS	6-311+G(2d)
Silane derivatives (**1**–**14**)	9.3	6.9	4.5	10.1	6.8	4.9	8.4	5.6	4.4
Pentacoordinate (**14**–**25**)	24.0	9.6	5.8	25.0	11.6	7.7	21.9	9.3	5.7
Hexacoordinate (**26**–**41**)	39.4	7.3	9.0	41.3	9.0	8.0	42.7	10.0	7.9

© 2011 Wiley-VCH Verlag GmbH & Co. KGaA, Weinheim

Table 4. MAE in ppm of calculated chemical shifts for molecules **1**–**10** and **22**.

HF/LDBS	MP2/LDBS	B3LYP/LDBS	BPW91/LDBS	HCTH407/LDBS
3.9	4.6	7.8	6.1	5.6

again observed for the HCTH407 functional, see Table 4). Importantly, the MP2 results offer large improvements for three previously discussed outliers included in these calculations (i.e. **1**, **10** and **22**). For the tetravalent molecules considered, the ^{29}Si NMR shieldings calculated at the HF/LDBS level of theory are in especially good agreement with the experimental data.

Conclusions

DFT/GIAO ^{29}Si NMR shielding calculations provided mostly satisfactory results for a set of 41 different molecules compared to the experimental data. With an MAE of 5.9 ppm, HCTH407/6-311+G(2d) consistently performs best among the different levels of theory employed in this work. Our study focused on medium-sized compounds with at least one hypervalent silicon atom and investigated a selection of 27 structurally diverse penta- and hexacoordinate compounds. It is evident that employment of a larger basis set than 6-31G(d,p) is necessary in order to obtain useful results for this class of molecules. Fortunately, employment of an LDBS offers a dramatic improvement at small additional computational costs. In this study, the choice of basis set exerted a much larger influence on the accuracy of the results than the choice of functional. Employment of the larger 6-311+G(2d) basis set on all atoms resulted in further improvements and furnished acceptable results for both tetravalent and hypervalent compounds. Nevertheless, a final note of caution is still warranted, as large differences between calculated and experimental shifts were observed in a few cases, such as compounds with Si–H bonds. Furthermore, GIAO-HF and MP2 ab initio calculations carried out for a smaller subset of compounds yielded better results than the DFT calculations (MAEs for HF, MP2 and HCTH407 were 3.9, 4.6 and 5.6 ppm, respectively). Of course, even for **22** with only 275 basis functions by using the LDBS, the MP2 calculations required 80–110 times more CPU time than the corresponding DFT calculations. This is already more favourable than expected, given the roughly N^5 scaling behaviour of the MP2 method.

Table 5. ^{29}Si NMR chemical shifts relative to TMS of 41 molecules and absolute isotropic shielding constants for TMS.

		Exp. shift	B3LYP			BPW91			HCTH407			Ref.
			6-31G(d,p)	LDBS	6-311+G(2d)	6-31G(d,p)	LDBS	6-311+G(2d)	6-31G(d,p)	LDBS	6-311+G(2d)	
1	Trimethoxysilane	–54.9 ($CDCl_3$)	–53.0	–66.5	–72.9	–50.2	–64.9	–68.6	–55.7	–68.2	–72.1	[40]
2	Ethyltrimethylsilane	1.6 (10% $CDCl_3$)	5.1	6.6	2.9	5.4	3.6	3.0	4.9	2.8	4.9	[41]
3	Hydroxymethyltrimethylsilane	–2.5 (10% $CDCl_3$)	2.2	3.3	–1.3	1.7	–0.1	–2.0	2.2	0.1	–1.7	[42]
4	Hexamethylsilacyclopropane	–49.3 ([D_8]THF)	–48.0	–53.5	–63.2	–48.9	–58.1	–63.7	–50.9	–56.3	–63.1	[43]
5	Diethyldimethylsilane	5.0 (10% $CDCl_3$)	7.8	8.8	3.9	7.6	5.4	3.8	7.8	4.8	3.2	[41]
6	1,1′-Dimethylsilacyclobutane	18.9 (10% $CDCl_3$)	20.7	23.6	21.3	21.3	20.4	20.8	18.4	18.6	19.4	[44]
7	Tetraethylsilane	6.5 (10% CDCl3)	14.9	14.2	8.3	14.3	10.2	8.5	14.7	8.8	7.1	[41]
8	Trimethylphenylsilane	–5.1 (10% $CDCl_3$)	3.2	–0.4	–5.6	3.5	–3.2	–5.3	3.3	–3.5	–5.8	[45]
9	Methoxytrimethylsilane	17.0 (10% $CDCl_3$)	17.5	23.3	17.1	21.0	23.3	21.2	17.1	18.4	16.5	[46]
10	Triethoxyphenylsilane	–55.6 ($CDCl_3$)	–53.3	–73.4	–81.0	–53.3	–72.8	–77.9	–54.4	–75.5	–80.9	[47]
11	Chloro-bis[(pyridin-2-yl-trimethylsilyl)methyl]methyl***silane***	22.9 (C_6D_6)	45.9	33.8	27.3	45.8	33.3	26.9	41.2	31.2	24.9	[48]
	Chloro-bis[(pyridin-2-yl-trimethyl***silyl***)methyl]methylsilane	1.5 (C_6D_6)	12.2, 12.5	8.2, 9.1	3.4, 5.2	13.8, 14.0	9.2, 10.1	4.5, 6.4	12.7, 12.9	9.5, 10.4	4.4, 6.4	
12	Bis[(pyridin-2-yltrimethylsilyl)methyl]dimethyl***silane***	3.2 (C_6D_6)	19.6	11.6	7.5	18.7	11.3	7.8	17.8	11.6	8.1	[48]
	Bis[(pyridin-2-yltrimethyl***silyl***)methyl]dimethylsilane	0.8 (C_6D_6)	11.3	6.0	2.9	11.2	5.9	3.1	9.9	5.9	2.7	
13	1,3-[2′,6′-Pyridinebis(methyleneoxy)]-1,3-bis(diphenyl)cyclodisiloxane	–41.6 ($CDCl_3$)	–13.3	–33.2	–41.0	–11.9	–30.1	–36.9	–15.0	–33.8	–40.7	[49]
14	1,3,10,12-Tetraoxo-2,11-(dimethylsilylene)[5.5]paracyclophane	–2.3 ($CDCl_3$)	3.7	0.02	–4.4	6.4	4.1	0.5	1.9	–1.5	–5.0	[50]
15	[Ethylene-*N*-2-hydroxyacetophenoniminato-*N*′-1-(2-hydroxyphenylato)vinylaminato]phenylsilane	–116.1	–83.6	–111.8	–119.4	–83.5	–110.3	–115.2	–83.8	–110.9	–116.0	[51]

© 2011 Wiley-VCH Verlag GmbH & Co. KGaA, Weinheim

Table 5. *(Continued)*.

		Exp. shift	B3LYP			BPW91			HCTH407			Ref.
			6-31G(d,p)	LDBS	6-311+G(2d)	6-31G(d,p)	LDBS	6-311+G(2d)	6-31G(d,p)	LDBS	6-311+G(2d)	
16	*N*-(Trifluorosilylmethyl)-glutarimide	–75.7 (CD_2Cl_2)	–53.1	–71.9	–74.2	–46.9	–64.2	–65.3	–52.7	–70.1	–71.1	[51]
17	Dichloro[(6-methylpyridin-2-yl)-bis(trimethylsilyl)-methyl]***silane***	–64.82 (C_6D_6)	–7.55	–31.6	–37.9	–7.6	–32.3	–37.7	–12.3	–32.0	–37.9	[48]
	Dichloro[(6-methylpyridin-2-yl)-bis(trimethyl***silyl***)-methyl]silane	1.94 (C_6D_6)	15.3, 13.7	8.3, 5.9	5.5, 3.0	14.8, 12.9	7.9, 5.3	5.4, 2.7	13.9, 11.0	8.1, 5.6	5.4, 2.5	
18	2,6-Pyridinebis(1,1-diphenylethoxy)diphenylsilane	–61.9 ($CDCl_3$)	–28.7	–56.2	–63.5	–28.9	–54.6	–60.8	–32.8	–56.9	–63.1	[49]
19	2,6-Pyridinebis(1,1-di-*p*-bromophenylmethoxy)-dimethylsilane	–56.5 ($CDCl_3$)	–36.1	–47.9	–54.0	–32.1	–41.9	–46.9	–34.6	–44.8	–50.4	[50]
20	3,3,7,7-Tetrakis-(4-fluorophenyl)-5-methyl-5-phenyl-4,6-dioxa-13-aza-5-silabicyclo[7.3.1]trideca-1(12),9(13),10-triene	–48.9 ($CDCl_3$)	–26.9	–44.0	–50.5	–26.5	–42.1	–47.5	–30.8	–45.0	–50.8	[52]
21	3,3,7,7-Tetrakis-(4-fluorophenyl)-5,5-dimethy-4,6-dioxa-13-aza-5-silabicyclo[7.3.1]trideca-1(12),9(13),10-triene	–31.7 ($CDCl_3$)	–12.9	–22.0	–27.6	–11.2	–19.0	–23.8	–16.0	–23.5	–28.2	[52]
22	Chlorodimethyl(3,4,7,8-tetrahydro-2*H*,6*H*-pyrimido[1,2-*a*]pyrimidin-1-ylmethyl-C^1,N^9)silicon	–49.1 (C_6D_6)	–51.6	–63.1	–67.5	–52.3	–62.4	–66.5	–51.2	–60.5	–64.3	[53]
23	2,6-Pyridinebis-(1,1-diphenylethoxy)dimethylsilane	–31.4 ($CDCl_3$)	–14.5	–23.7	–29.1	–12.8	–20.6	–25.2	–17.4	–29.7	–25.1	[54]
24	2,6-Bis[2-oxy(2-adamantylidine)]ethylpyridinedimethylsilicon	–41.9 ($CDCl_3$)	–21.9	–32.4	–38.5	–21.2	–30.2	–35.6	–25.8	–34.0	–39.4	[55]
25	[Trimethylen-*N*-2-oxyacetophenoneiminato-*N′*-1-(2-oxyphenylato)vinylaminato]phenylsilane	–107.7 ($CDCl_3$)	–67.0	–94.5	–103.0	–67.2	–93.2	–99.9	–69.0	–94.7	–101.4	[56]
26	Ethylene-*N*,*N′*-bis-(2-oxy-acetophenoneiminato)-8-oxyquinolinatophenylsilane	–181.3 ($CDCl_3$)	–135.9	–189.2	–192.0	–142.3	–180.5	–185.3	–140.3	–178.2	–183.5	[56]
27	Benzoato[ethylene-*N*,*N′*-bis(2-oxyacetophenoneiminato)]phenylsilane	–186	–149.8	–187.9	–196.1	–149.1	–185.1	–190.0	–144.9	–182.4	–188.3	[56]
28	Benzoatobis(*N*-benzyl-2-oxyacetophenoneiminato)phenylsilicon	–183.4 ($CDCl_3$)	–145.3	–184.7	–192.3	–143.7	–185.8	–181.6	–141.9	–178.9	–184.0	[56]
29	Fluorobis(*N*-benzyl-2-oxyacetophenoneiminato)phenylsilicon	–180.9 ($CDCl_3$)	–143.5	–180.6	–188.2	–140.9	–177.4	–180.6	–139.6	–175.8	–179.8	[56]
30	Benzoato[trimethylene-*N*,*N′*-bis(2-oxyacetophenoneiminato)]-phenylsilane	–184.2 ($CDCl_3$)	–147.5	–186.2	–189.5	–146.7	–181.7	–183.2	–143.7	–178.8	–181.5	[56]
31	[Ethylene-*N*,*N′*-bis(2-oxyacetophenoneiminato)]-2,4,6-trinitrophenolatophenylsilane	–172	–138.7	–175.5	–181.5	–135.8	–171.7	–173.3	–134.8	–170.0	–173.2	[56]
32	[Ethylene-*N*,*N′*-bis(2-oxyacetophenoneiminato)]-2-(5-phenyltetrazolido)-(phenyl)silicon	–175.6 (DMSO)	–143.9	–184.2	–188.7	–143.7	–181.7	–182.6	–140.9	–179.0	–181.2	[56]
33	Dichloro-bis(*N*-methylpropionamido)-silicon	–159.9	–123.4	–157.1	–162.9	–121.2	–151.8	–157.0	–119.5	–150.3	–155.5	[57]
34	Dichlorobis[*N*-(isopropylideneimino)phenylacetimidato-*N*,*O*]silicon	–163.7 ($CDCl_3$)	–114.6	–150.9	–157.1	–110.0	–143.8	–149.3	–110.9	–142.1	–147.3	[58]

© 2011 Wiley-VCH Verlag GmbH & Co. KGaA, Weinheim

Table 5. *(Continued)*.

		Exp. shift	B3LYP			BPW91			HCTH407			Ref.
			6-31G(d,p)	LDBS	6-311+G(2d)	6-31G(d,p)	LDBS	6-311+G(2d)	6-31G(d,p)	LDBS	6-311+G(2d)	
35	(2,2′-Bipyridyl)trifluoro-(phenylethynyl)silane	–178.7 ($CDCl_3$)	–131.4	–171.4	–174.7	–126.2	–162.7	–164.9	–124.7	–162.9	–165.5	[59]
36	Hexakis(azido)-silicate	–188.7 (CH_3CN)	–161.5	–201.4	–206.1	–160.6	–195.1	–199.5	–157.3	–192.3	–197.8	[60]
37	Bis[*N*-(dimethylamino)-trifluoroacetimidato-*N*,*O*]phenyl(trifluoro-methanesulfonato)-silicon	–140.6 (CD_2Cl_2)	–100.6	–138.7	–142.1	–96.8	–130.8	–138.1	–96.0	–129.5	–132.8	[61]
38	Bis[*N*-(dimethyl-amino)benzimidato-*N*,*O*](catecholato-*O*,*O*)silicon	–141.0 ([D_8]toluene)	–101.1	–138.0	–143.3	–95.6	–128.7	–132.8	–95.8	–128.9	–133.2	[62]
39	[Si(salen*)Me(NCS)]	–170.8 ($CDCl_3$)	–154.6	–188.9	–193.9	–154.1	–184.1	–188.3	–149.9	–181.1	–185.4	[63]
40	Bis(4-methylpyridine)-methylhydridodichloro-silane	–135.6	–96.2	–129.2	–135.9	–93.6	–125.9	–131.8	–95.2	–121.6	–127.3	[64]
41	Trichlorotris(hexa-methylphosphorictri-amide)silicon	–205.8 ([D_8]toluene)	–129.6	–179.5	–184.8	–126.4	–172.9	–177.2	–129.2	–171.2	–176.5	[20]
	Tetramethylsilane	0	412.7	331.9	327.0	403.2	329.8	325.6	402.2	342.0	337.7	

Table 6. ^{29}Si NMR chemical shifts relative to TMS at higher levels of theory for six outliers, and absolute isotropic shielding constants for TMS.

		Exp. shift	HCTH407/6-311+G(2d)//B3LYP/6-31G(d,p)	HCTH407/6-311+G(2d)//HCTH407/6-311+G(2d)	HCTH407/6-311++G(2df,2pd)//HCTH407/6-311+G(2d)	HCTH407/6-311+G(2d)//HCTH407/6-311+G(2d) with IEF-PCM
1	Trimethoxysilane	–54.9 ($CDCl_3$)	–72.1	–74.5	–75.3	–72.7
10	Triethoxyphenylsilane	–55.6 ($CDCl_3$)	–80.9	–83.8	–85.7	–79.6
17	Dichloro[(6-methyl-pyridin-2-yl)-bis(trimethylsilyl)methyl]***silane***	–64.82 (C_6D_6)	–38.0	–50.2	–49.8	–55.1
	Dichloro[(6-methylpyridin-2-yl)-bis(trimethyl***silyl***)methyl]silane	1.94 (C_6D_6)	5.4, 2.5	5.3, 3.6	6.1, 5.1	5.2, 3.9
22	Chlorodimethyl(3,4,7,8-tetrahydro-2*H*,6*H*-pyrimido[1,2-*a*]-pyrimidin-1-ylmethyl-C^1,N^9)silicon	–49.1 (C_6D_6)	–64.3	–59.2	–58.2	–55.5
34	Dichloro-bis-[*N*-(isopropylidene-imino)phenyl-acetimidato-*N*,*O*]silicon	–163.7 ($CDCl_3$)	–147.3	–142.4	–141.0	–142.9
41	Trichlorotris-(hexamethylphosphoric-triamide)-silicon	–205.8 ([D_8]toluene)	–176.5	–168.8	–166.3	–170.9
MAE			16.7	16.9	17.9	14.8
	Tetramethylsilane		337.7	337.7	339.0	338.2

Computational Details

For ^{29}Si NMR shielding calculations, DFT calculations were carried out by using the GIAO method in conjunction with the hybrid B3LYP[29] functional, the generalized gradient approximation functional (GGA) BPW91[30,31] and the *meta*-GGA functional HCTH407. The choice of functionals was motivated by the findings of Apeloig et al.[13] and allows for a convenient comparison with their published results. Three different basis sets were used for ^{29}Si NMR shielding calculations: Pople's double-zeta, split-valence basis set 6-31G(d,p) with additional polarization functions on all atoms; the triple-zeta, split-valence basis set 6-311+G(2d) with additional diffuse and polarization functions only on heavy atoms; a combination thereof, with 6-31G(d,p) on all atoms except Si, where 6-311+G(2d) was used, which for the purpose of this study is referred to as LDBS.[32–34] The basis sets and references for all Pople-type basis sets used in this study are provided at https://bse.pnl.gov/bse/portal. Additional ab initio calculations were carried out by using second-order Møller-Plesset perturbation theory (MP2) with all electrons included in the correlation calculation.[35,36]

To facilitate the comparison of calculated and experimental chemical shifts, the calculated isotropic shielding constants were converted into chemical shifts by using tetramethylsilane (TMS) as a reference. To this end, the shielding constants for TMS were calculated at every level of theory used in the study (see Tables 5 and 6). All geometries were optimized at the B3LYP/6-31G(d,p) level of theory, which is known to produce reliable results with regard to the convergence of structural parameters.[37,38] Where available (compounds **11**–**41**), geometry optimizations were started from structures obtained from the Cambridge Crystallographic Data Centre (www.ccdc.cam.ac.uk/data request/cif) or the Inorganic Crystal Structure Database FIZ Karlsruhe. Where appropriate, symmetry constraints were applied (i.e. when the experimentally available NMR shifts indicated the presence of molecular symmetry). All calculations were carried out with the Gaussian 03 suite of programs (revision D.01).[39]

Supporting Information (see footnote on the first page of this article): Cartesian coordinates of the calculated geometries and structural formulae of all compounds.

---

[1] M. Bühl, M. Kaupp, O. L. Malkina, V. G. Malkin, *J. Comput. Chem.* **1999**, *20*, 91–105.
[2] J. C. Facelli, in *Modern Magnetic Resonance* (Eds.: G. A. Webb), Springer, The Netherlands, **2006**.
[3] N. F. Ramsey, *Phys. Rev.* **1950**, *78*, 699–703.
[4] K. Wolinski, J. F. Hinton, P. Pulay, *J. Am. Chem. Soc.* **1990**, *112*, 8251–8260.
[5] G. Schreckenbach, T. Ziegler, *J. Phys. Chem.* **1995**, *99*, 606–611.
[6] G. Rauhut, S. Puyear, K. Wolinski, P. Pulay, *J. Phys. Chem.* **1996**, *100*, 6310–6316.
[7] M. Kaupp, V. G. Malkin, O. L. Malkina, *Encyclopedia of Computational Chemistry*, Wiley, New York, **1998**.
[8] M. Kaupp, O. L. Malkina, V. G. Malkin, *J. Chem. Phys.* **1997**, *106*, 9201–9219.
[9] T. Heine, A. Goursot, G. Seifert, J. Weber, *J. Phys. Chem. A* **2001**, *105*, 620–626.
[10] C. Corminbœuf, T. Heine, J. Weber, *Chem. Phys. Lett.* **2002**, *357*, 1–7.
[11] J. Sefcik, W. A. Goddard, *Geochim. Cosmochim. Acta* **2001**, *65*, 4435–4443.
[12] T. B. Casserly, K. K. Gleason, *J. Phys. Chem. B* **2005**, *109*, 13605–13610.
[13] M. Karni, Y. Apeloig, N. Takagi, S. Nagase, *Organometallics* **2005**, *24*, 6319–6330.
[14] A. D. Boese, N. C. Handy, *J. Chem. Phys.* **2001**, *114*, 5497–5503.
[15] J. Gauss, *Chem. Phys. Lett.* **1992**, *191*, 614–620.
[16] J. Ambati, S. E. Rankin, *J. Phys. Chem. A* **2010**, *114*, 5279–5286.
[17] R. R. Holmes, *Chem. Rev.* **1996**, *96*, 927–950.
[18] M. G. Voronkov, O. M. Trofimova, Y. I. Bolgova, N. F. Chernov, *Russ. Chem. Rev.* **2007**, *76*, 825–845.
[19] D. Kost, I. Kalikhman, *Acc. Chem. Res.* **2009**, *42*, 303–314.
[20] V. A. Du, S. O. Baumann, G. N. Stipicic, U. Schubert, *Z. Naturforsch. B* **2009**, *64*, 1553–1557.
[21] D. H. Brouwer, I. L. Moudrakovski, R. J. Darton, R. E. Morris, *Magn. Reson. Chem.* **2010**, *48*, 113–121.
[22] D. A. Forsyth, A. B. Sebag, *J. Am. Chem. Soc.* **1997**, *119*, 9483–9494.
[23] I. Alkorta, J. Elguero, *Struct. Chem.* **1998**, *9*, 187–202.
[24] T. A. Ruden, K. Ruud, *Calculations of NMR and EPR Parameters – Theory and Applications*, Wiley, Weinheim, **2004**.
[25] M. T. Cancès, B. Mennucci, J. Tomasi, *J. Chem. Phys.* **1997**, *107*, 3032–3037.
[26] M. Cossi, V. Barone, B. Mennucci, J. Tomasi, *Chem. Phys. Lett.* **1998**, *286*, 253–260.
[27] B. Mennucci, J. Tomasi, *J. Chem. Phys.* **1997**, *106*, 5151–5158.
[28] T. Heine, A. Goursot, G. Seifert, J. Weber, *J. Phys. Chem. A* **2001**, *105*, 620–626.
[29] P. J. Stephens, F. J. Devlin, C. F. Chabalowski, M. J. Frisch, *J. Phys. Chem.* **1994**, *98*, 11623–11627.
[30] A. D. Becke, *J. Phys. Chem.* **1992**, *97*, 9173–9177
[31] J. P. Perdew, Y. Wang, *Phys. Rev. B* **1992**, *45*, 13244–13249.
[32] D. Chesnut, K. D. Moore, *J. Comput. Chem.* **1989**, *10*, 648–659.
[33] D. Chesnut, B. Rusiloski, K. Moore, D. Egolf, *J. Comput. Chem.* **1993**, *14*, 1364–1375.
[34] D. Chesnut, *Chem. Phys.* **1996**, *213*, 153–158.
[35] J. Gauss, *J. Chem. Phys.* **1993**, *99*, 3629–3643.
[36] J. Gauss, *Phys. Chem. Chem. Phys.* **1995**, *99*, 1001–1010.
[37] F. A. Hamprecht, A. J. Cohen, D. J. Tozer, N. C. Handy, *J. Chem. Phys.* **1998**, *109*, 6264–6271.
[38] V. N. Staroverov, G. E. Scuseria, J. Tao, J. P. Perdew, *J. Chem. Phys.* **2003**, *119*, 12129–12137.
[39] M. J. Frisch, G. W. Trucks, H. B. Schlegel, G. E. Scuseria, M. A. Robb, J. R. Cheeseman, G. Scalmani, V. Barone, B. Mennucci, G. A. Petersson, H. Nakatsuji, M. Caricato, X. Li, H. P. Hratchian, A. F. Izmaylov, J. Bloino, G. Zheng, J. L. Sonnenberg, M. Hada, M. Ehara, K. Toyota, R. Fukuda, J. Hasegawa, M. Ishida, T. Nakajima, Y. Honda, O. Kitao, H. Nakai, T. Vreven, J. A. Montgomery Jr., J. E. Peralta, F. Ogliaro, M. Bearpark, J. J. Heyd, E. Brothers, K. N. Kudin, V. N. Staroverov, R. Kobayashi, J. Normand, K. Raghavachari, A. Rendell, J. C. Burant, S. S. Iyengar, J. Tomasi, M. Cossi, N. Rega, J. M. Millam, M. Klene, J. E. Knox, J. B. Cross, V. Bakken, C. Adamo, J. Jaramillo, R. Gomperts, R. E. Stratmann, O. Yazyev, A. J. Austin, R. Cammi, C. Pomelli, J. W. Ochterski, R. L. Martin, K. Morokuma, V. G. Zakrzewski, G. A. Voth, P. Salvador, J. J. Dannenberg, S. Dapprich, A. D. Daniels, Ö. Farkas, J. B. Foresman, J. V. Ortiz, J. Cioslowski, and D. J. Fox, *Gaussian 03*, Revision D.01, Gaussian, Inc., Wallingford, CT, **2004**.
[40] J. J. C. Chrusciel, *Polymer* **2005**, *516*, 508–516.
[41] J. Schraml, V. Chvalovsky, M. Magi, E. Lippmaa, *Collect. Czech. Chem. Commun.* **1979**, *44*, 854–865.
[42] J. Schraml, V. Chvalovsky, M. Magi, E. Lippmaa, *Collect. Czech. Chem. Commun.* **1978**, *43*, 3365–3372.
[43] D. Seyferth, D. C. Annarelli, S. C. Vick, D. P. Duncan, *J. Organomet. Chem.* **1980**, *201*, 179–195.
[44] A. M. Krapivin, *Izv. Akad. Nauk Ser. Khim.* **1980**, *7*,1950–1951.
[45] J. Schraml, J. Pola, H. Jancke, G. Engelhardt, M. Cerny, V. C. Chvalovsky, *Collect. Czech. Chem. Commun.* **1976**, *41*, 360–367.
[46] J. Schraml, *Collect. Czech. Chem. Commun.* **1981**, *46*, 377–390.

© 2011 Wiley-VCH Verlag GmbH & Co. KGaA, Weinheim

[47] V. A. Pestunovich, S. N. Tandura, M. G. Voronkov, G. Engelhardt, E. Lippmaa, T. Pehk, V. F. Sidorkin, G. Zelcans, V. P. Baryshok, *Izv. Akad. Nauk Ser. Khim.* **1978**, *240*, 914–917.

[48] T. van den Ancker, C. Raston, B. W. Skelton, A. H. White, *Organometallics* **2000**, *19*, 4437–4444.

[49] E. Gómez, V. Santes, V. La Luz, N. de Farfan, *J. Organomet. Chem.* **1999**, *590*, 237–241.

[50] E. Gómez, V. Santes, V. La Luz, N. de Farfan, *J. Organomet. Chem.* **2001**, *622*, 54–60.

[51] M. G. Voronkov, O. M. Trofimova, N. F. Chernov, Y. I. Bolgova, A. I. Albanov, N. N. Chipanina, E. A. Zelbst, *Heteroat. Chem.* **2006**, *17*, 567–571.

[52] E. Gómez, Z. Hernandez, C. Alvarez-Toledano, R. A. Toscano, V. Santes, P. J. Scharma, *J. Organomet. Chem.* **2002**, *648*, 280–287

[53] D. Kummer, S. H. Abdel Halim, *J. Organomet. Chem.* **1993**, *446*, 51–65.

[54] T. K. Prakasha, A. Chandrasekaran, R. O. Day, R. R. Holmes, *Inorg. Chem.* **1996**, *35*, 4342–4346.

[55] J. J. H. Edema, R. Libbers, A. Ridder, R. M. Kellogg, A. L. Spek, *J. Organomet. Chem.* **1994**, *464*, 127–131.

[56] J. Wagler, U. Bohme, E. Brendler, B. Thomas, S. Goutal, H. Mayr, B. Kempf, G. Remennikov, G. Roewer, *Inorg. Chim. Acta* **2005**, *358*, 4270–4286.

[57] J. Yang, J. Verkade, *J. Organomet. Chem.* **2002**, *651*, 15–21.

[58] I. Kalikhman, B. Gostevskii, O. Girshberg, A. Sivaramakrishna, N. Kocher, D. Stalke, D. Kost, *J. Organomet. Chem.* **2003**, *686*, 202–214.

[59] M. Nakash, M. Goldvaser, I. Goldberg, *Inorg. Chem.* **2004**, *43*, 5792–5794.

[60] A. C. Filippou, P. Portius, G. Schnakenburg, *J. Am. Chem. Soc.* **2002**, *124*, 12396–12397.

[61] D. Kost, V. Kingston, B. Gostevskii, A. Ellern, D. Stalke, B. Walfort, I. Kalikhman, *Organometallics* **2002**, *21*, 2293–2305.

[62] I. Kalikhman, V. Kingston, O. Girshberg, D. Kost, *Organometallics* **2001**, *20*, 4713–4720.

[63] G. González-García, E. Alvarez, A. Marcos-Fernández, J. A. Gutiérrez, *Inorg. Chem.* **2009**, *48*, 4231–4238.

[64] G. W. Fester, J. Wagler, E. Brendler, U. Böhme, D. Gerlach, E. Kroke, *J. Am. Chem. Soc.* **2009**, *131*, 6855–6864.

Received: March 22, 2011
Published Online: July 4, 2011